Biochemical and Biophysical Research Communications 432 (2013) 707–712

Contents lists available at SciVerse ScienceDirect

Biochemical and Biophysical Research Communications

journal homepage: www.elsevier.com/locate/ybbrc

Negatively charged residues (Asp378 and Asp379) in the last ten amino acids of the C-terminal tail of Cx43 hemichannels are essential for loop/tail interactions

Catheleyne D'hondt [a], Jegan Iyyathurai [a], Nan Wang [b], Robert G. Gourdie [c], Bernard Himpens [a], Luc Leybaert [b], Geert Bultynck [a,*]

[a] Laboratory of Molecular and Cellular Signalling, Department Cellular and Molecular Medicine, Campus Gasthuisberg O/N-1 Bus 802, Herestraat 49, BE-3000 Leuven, Belgium
[b] Department of Basic Medical Sciences, Physiology Group, Faculty of Medicine and Health Sciences, Ghent University, Ghent, Belgium
[c] Department of Regenerative Medicine and Cell Biology, Cardiovascular Developmental Biology Center, Medical University of South Carolina, Charleston, SC 29425, USA

ARTICLE INFO

Article history:
Received 11 January 2013
Available online 29 January 2013

Keywords:
Connexin
Hemichannels
Peptides
ATP release
Ca^{2+}-wave propagation

ABSTRACT

Connexin 43 (Cx43)-hemichannel activity is controlled by intramolecular interactions between cytoplasmic loop and C-terminal tail. We previously identified the last 10 amino acids of the C-terminal tail of Cx43 as essential for Cx43-hemichannel activity. We developed a cell-permeable peptide covering this sequence (TAT-Cx43CT). In this study, we examined the critical molecular determinants in TAT-Cx43CT to restore Cx43-hemichannel activity. Using amino acid substitutions in TAT-Cx43CT, we identified the two aspartate (Asp378 and Asp379) and two proline (Pro375 and Pro377) residues as critical for TAT-Cx43CT activity, since TAT-Cx43CT$^{DD/AA}$ and TAT-Cx43CT$^{PP/GG}$ did not overcome the inhibition of Cx43-hemichannel activity induced by thrombin, micromolar cytoplasmic Ca^{2+} concentration or truncation of Cx43 at M^{239}. Consistent with this, we found that biotin-Cx43CT$^{DD/AA}$ was much less efficient than biotin-Cx43CT to bind the purified CL domain of Cx43 in surface plasmon resonance experiments. In conclusion, we postulate that Asp378 and Asp379 in the C-terminal part of Cx43 are essential for loop/tail interactions in Cx43 hemichannels, while Pro375 and Pro377 may help to properly coordinate the critical Asp residues.

1. Introduction

Connexins (Cx) control intercellular communication by coordinating multicellular responses in organs, via chemical or electrical signals [1–3]. Six Cx subunits assemble into a connexon, which can exist as free, unopposed hemichannels or as head-by-head apposed hemichannels that form gap junctions [4,5]. While gap junctions provide a direct signaling pathway between neighboring cells, hemichannels mediate paracrine signaling, by releasing signaling molecules like ATP that act on neighboring cells expressing purinergic receptors [4,6,7]. This results in intracellular Ca^{2+} signals in neighboring cells, initiating intercellular Ca^{2+}-waves that propagate between several rows of cells [8–12]. Also, cytosolic [Ca^{2+}] rises in the physiological range (0.5–1 μM) trigger Cx-hemichannel opening [13–15]. Thus, physiological agonists that trigger intracellular Ca^{2+} oscillations provoke Cx-hemichannel opening [16]. Cx43 hemichannels also mediate the release of gliotransmitters from astrocytes in the basal amygdala, establishing fear-memory consolidation [17]. Corneal endothelial cells of bovine origin have been used in our laboratory as a model system for studying Cx43-hemichannel activity [9,10,18–24]. Using mechanical stimulation (MS)-induced intercellular Ca^{2+}-wave propagation experiments, we found that (i) Cx43 is the major Cx isoform mediating intercellular communication [24], and (ii) paracrine signaling via hemichannel-mediated ATP release accounts for the majority of the cell-to-cell propagation mechanism of these waves [9,10]. We also found that thrombin inhibits Cx43-hemichannel-driven intercellular Ca^{2+}-wave propagation by activating the contractile system [18,22]. The inhibition involved a disturbance of intramolecular interactions between the cytoplasmic loop and C-terminal tail [24], essential for Cx43-hemichannel activity. Cx43 lacking its C-terminal tail ($Cx43^{M239}$) does not display hemichannel activity, while a cell-permeable peptide corresponding to the last 10 amino acids (aa) of the C-terminal tail (TAT-Cx43CT) could restore $Cx43^{M239}$-hemichannel activity. Similarly, thrombin-induced inhibition of Cx43-hemichannel activity in corneal endothelial cells was completely suppressed by TAT-Cx43CT. Cx43CT was able to directly interact with the L2 region of the cytoplasmic loop of Cx43. These results indicated that the last 10 aa of the C-terminal tail of Cx43 are essential for Cx43-hemichannel opening activity [25]. Yet, the molecular determinants in Cx43CT responsible for establishing functional Cx43 hemichannels have not been resolved yet. Here, we established which aa in the Cx43CT peptide were critical for Cx43-hemichannel opening.

* Corresponding author. Fax: +32 16 345991.
E-mail address: geert.bultynck@med.kuleuven.be (G. Bultynck).

0006-291X/$ - see front matter © 2013 Elsevier Inc. All rights reserved.
http://dx.doi.org/10.1016/j.bbrc.2013.01.066

2. Materials and methods

2.1. Cell culture

Cultures of primary bovine corneal endothelial cells (BCECs) from fresh eyes were established as described previously [9,10,18–24]. HeLa cells ectopically expressing either the full-length Cx43 or the CT-truncated mutant of Cx43 ($Cx43^{M239}$) were established as described previously [24,26].

2.2. Peptides

All synthetic peptides (>90% pure) were obtained from Thermo Fisher Scientific (Ulm, Germany; Table 1). TAT peptides were used at 100 μM incubated with the cells for 30 min at room temperature (RT).

2.3. Imaging of intercellular Ca^{2+}-wave propagation

Intercellular Ca^{2+}-wave propagation was assayed in Fluo4-loaded (10 μM for 30 min at 37 °C) BCEC as described previously [9,10,18–24]. TAT peptides (100 μM) were present in the bath solution during Fluo-4 loading. After washing the cells, the dye was excited at 488 nm, and its fluorescence emission was collected at 530 nm. Spatial changes in $[Ca^{2+}]_i$ following point mechanical stimulation (MS) were measured with the confocal microscope (LSM510, Zeiss) using a 40X objective (Air, 1.2 N.A.). A point MS, applied to a single cell, consisted of an acute deformation of the cell by briefly touching less than 1% percent of the surface area of its cell membrane with a glass micropipette (tip diameter < 1 μm) coupled to a piezoelectric crystal (Piezo device P-280, Amplifier-E463; PI Polytech, Karlsruhe, Germany) mounted on a micromanipulator, as described previously [9,10,18–24]. Polygonal regions of interest (ROIs) were drawn to define the borders of each cell. Fluorescence was averaged over the area of each ROI. Normalized fluorescence (NF) was then obtained by dividing the fluorescence by the average fluorescence before MS. We quantified the propagation of the intercellular Ca^{2+} wave by measuring the total surface area of responsive cells (active area, AA) with NF $\geqslant$ 1.1, using imaging software (LSM Image 4.2; Zeiss).

2.4. ATP release

ATP release from BCEC was measured *via* a luciferin–luciferase system [18,20]. One hundred microliter samples were taken from the 500 μl bathing solution covering the cells and transferred to a custom-built photon counting set-up to measure the luminescence as described previously [9,10]. Briefly, photons emitted as a result of the oxidation of luciferin in the presence of ATP and O_2 and catalyzed by luciferase were detected by a photon counting photomultiplier tube (H7360-01; Hamamatsu Photonics, Hamamatsu, Japan). Voltage pulses from the photomultiplier module were counted with a high-speed counter (PCI-6602; National Instruments, Austin, Texas, USA). Dark count of the photomultiplier tube was <80 counts/s.

ATP release from HeLa cells, ectopically expressing either Cx43 or $Cx43^{M239}$, was triggered by A23187 and measured *via* a luciferin-luciferase system [13]. Cellular ATP release was accumulated over the period of trigger exposure (5 min). Baseline measurements were performed on separate cultures using standard HBSS-HEPES. ATP release was normalized to the signal obtained in the absence of the trigger and is expressed as fold increase.

Table 1
Overview of the sequence of different TAT-fused peptides used in this study.

Name	Sequence
TAT-Cx43CT	TAT-SRPRPDDLEI
TAT-$Cx43CT^{DD/AA}$	TAT-SRPRPAALEI
TAT-$Cx43CT^{PP/GG}$	TAT-SRGRGDDLEI
TAT-$Cx43CT^{RR/AA}$	TAT-SAPAPDDLEI
TAT-Cx43CT reverse	TAT-SIELDDPRPR
Biotin-Cx43CT	Biotin-RQPKLWFPNRRKPWKKRPRPDDLEI
Biotin-Cx43CT reverse	Biotin-RQPKIWFPNRRKPWKKIELDDPRPR
Biotin-$Cx43CT^{DD/AA}$	Biotin-RQPKIWFPNRRKPWKKRPRPAALEI
Biotin-$Cx43CT^{DD/AA}$ reverse	Biotin-RQPKIWFPNRRKPWKKIELAAPRPR

2.5. Expression and purification of the CL domain

The CL domain of human Cx43 (aa 100–154) was cloned in the pGEX6p2 vector, yielding GST-CL with a PreScission-protease-cleavage site between GST and CL. GST-CL was purified from E. coli BL21(DE3) cells induced with 0.5 mM IPTG. The bacterial pellet was resuspended in cold lysis solution (20 mM Tris/HCl, pH 7.5, 500 mM NaCl, 1% Triton-X-100) containing protease inhibitors and cells were lysed by sonication. After removal of the cell debris by centrifugation, the soluble protein fraction was incubated with Glutathione-Sepharose 4B for 2 h at 4 °C. The beads were collected and washed three times with PBS and incubated with PreScission protease (GE Healthcare Life Sciences) in cleavage buffer (50 mM Tris–HCl, pH 7.0, 150 mM NaCl, 1 mM EDTA, 1 mM dithiothreitol) at 4 °C for 6 h. The protein was dialyzed against 1X DPBS without $CaCl_2$ and $MgCl_2$ (Gibco®, Life Technologies) using 2 kDa MWCO dialyzing cassette (Slide-A-Lyzer®, Thermo Fisher Scientific).

2.6. Surface plasmon resonance (SPR) experiments using biotin-Cx43CT

All binding experiments were performed using Biacore T200 instrument (GE Healthcare). Equal amounts (about 1300 resonance units) of >95% pure biotinylated peptides were immobilized on each flow cell of a streptavidin-coated sensor chip (Sensor Chip SA, Biacore Inc., Uppsala, Sweden) using HEPES buffer (in mM: 10 HEPES, 1 EDTA, 100 NaCl) with 0.005% polysorbate-20 (Tween-20) at pH 7.4. The Cx43CT peptide sequence (underlined aa) was fused to Biotin *via* a linker sequence (Table 1). Measurements with different [CL] as analyte were done in HEPES buffer (in mM: 10 HEPES, 100 NaCl, pH 7.4) at a flow rate of 30 μl/min in random order (injection volume 120 μl). Bound protein was removed by injection of 10 μl regeneration buffer (50 mM NaOH, 1 M NaCl) at 10 μl/min. Background signals obtained from the reference flow cell, containing the reversed biotinylated peptide, were subtracted to generate response curves.

2.7. Statistical analysis

All values represent mean ± S.E.M. For statistical analyses, each treatment was compared to its respective control, and significance was determined using a 1-way ANOVA. Differences were considered significant at $P < 0.05$. "*N*" indicates the number of days of experiments, while "*n*" represents the total number of independent experiments (the number of mechanically stimulated cells).

3. Results

3.1. Asp and Pro residues are essential for TAT-Cx43CT to prevent thrombin-inhibition of intercellular Ca^{2+}-waves in BCEC

MS results in the initiation and propagation of an intercellular Ca^{2+} wave in BCEC (Fig. 1A). The active area of the intercellular Ca^{2+} wave, corresponding to the maximal area covered by the

spreading of the Ca^{2+} wave, was quantified and normalized as a percentage of the area under control conditions (Fig. 1B). Treatment with thrombin led to a prominent inhibition of the active area ($N = 5$, $n = 50$) (Fig. 1). TAT-Cx43CT alleviated the inhibition of the active area by thrombin ($N = 5$, $n = 50$) (Fig. 1). Next, we assessed the activity of TAT-Cx43CT, in which we substituted the two Aspartate residues with two Alanine residues (TAT-Cx43CT$^{DD/AA}$), the two Proline residues with two Glycine residues (TAT-Cx43CT$^{PP/GG}$), or the two Arginine residues with two Alanine residues (TAT-Cx43CT$^{RR/AA}$) (Fig. 1). Importantly, TAT-Cx43CT$^{RR/AA}$ was equally potent in suppressing the thrombin-induced inhibition of the active area as TAT-Cx43CT ($N = 5$, $n = 50$) (Fig. 1). However, TAT-Cx43CT$^{DD/AA}$ and TAT-Cx43CT$^{PP/GG}$ did not alleviate this inhibition ($N = 5$, $n = 50$) (Fig. 1). This indicates that the two Aspartate and two Proline residues are essential for maintaining functional Cx43 hemichannels under conditions of enhanced contractility, while the Arg residues are dispensable.

3.2. Asp and Pro residues are essential for TAT-Cx43CT to overcome thrombin-inhibition of Cx43-hemichannel-mediated ATP release

In order to study if TAT-Cx43CT$^{DD/AA}$ and TAT-Cx43CT$^{PP/GG}$ could also overcome the thrombin-induced inhibition of Cx43-hemichannel-mediated ATP release associated with the

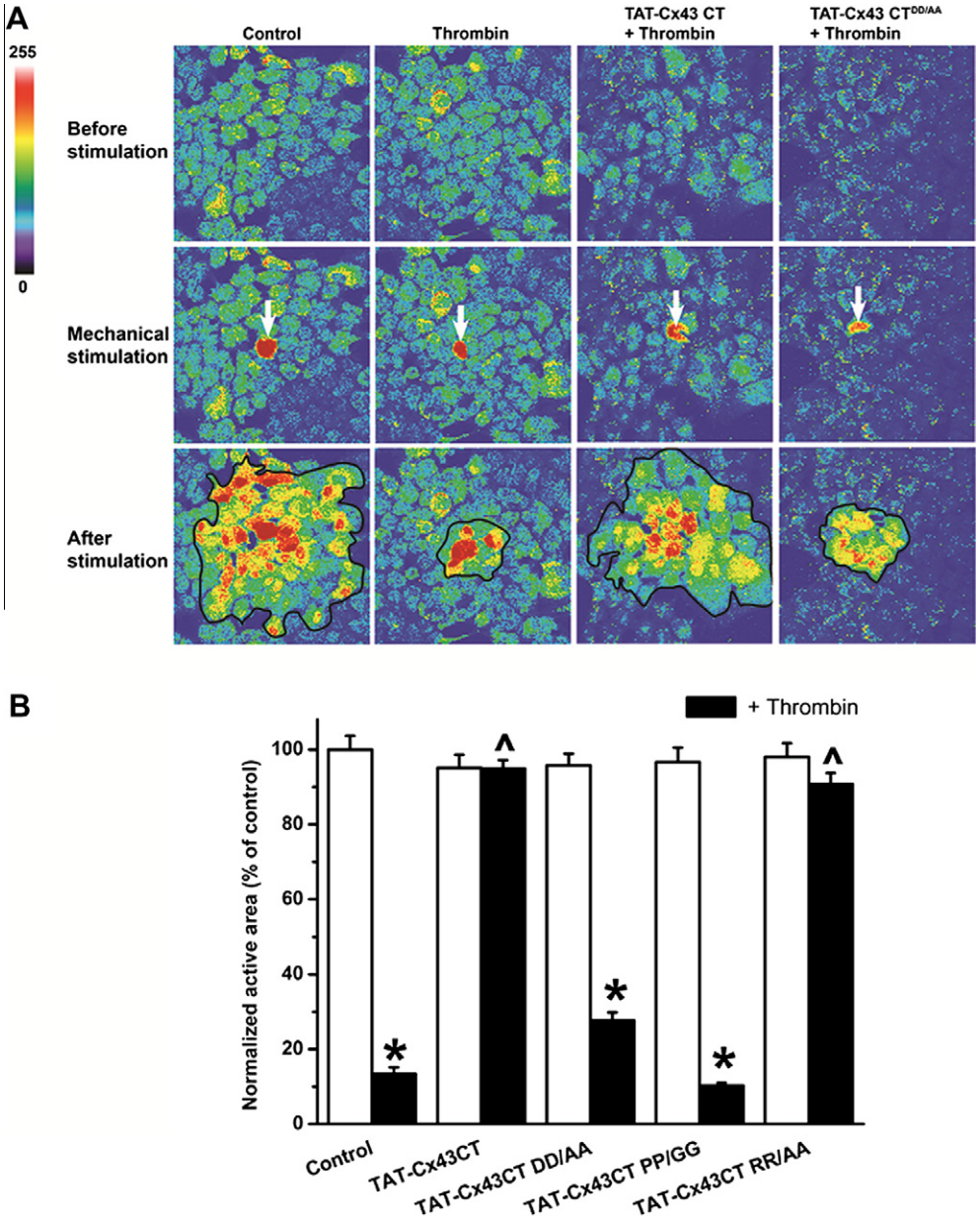

Fig. 1. Effect of thrombin on MS-induced intercellular Ca^{2+}-wave propagation in control condition and after exposure to TAT-Cx43CT or TAT-Cx43CT$^{DD/AA}$ in confluent BCEC. (A) Representative pseudocolored fluo-4 fluorescence Ca^{2+} images during and after MS in control condition and after exposure to TAT-Cx43CT or TAT-Cx43CT$^{DD/AA}$ in BCEC. The first image shows the fluorescence intensities before stimulation. The white arrow in the second image identifies the MS cell. The third image shows the maximal active area reached (black line). Note that some cells have already recovered from the Ca^{2+} change associated with the wave. (B) TAT-Cx43CT and TAT-Cx43CT$^{RR/AA}$, but not TAT-Cx43CT$^{DD/AA}$ and TAT-CX43CT$^{PP/GG}$, overcome thrombin-induced inhibition of Cx43-hemichannel-driven MS-induced intercellular Ca^{2+}-wave propagation in confluent BCEC. The normalized active area of MS-induced intercellular Ca^{2+}-wave propagation upon MS in untreated conditions or after thrombin-treatment is shown. These experiments were performed in control conditions or after exposure to TAT-Cx43CT, TAT-Cx43CT$^{DD/AA}$, TAT-CX43CT$^{PP/GG}$ or TAT-Cx43CT$^{RR/AA}$ ($N = 5$, $n = 50$). $*$ indicates a significant ($p < 0.001$) inhibition compared to control condition. ^ indicates that TAT-Cx43CT and TAT-Cx43CT$^{RR/AA}$ significantly ($p < 0.001$) alleviate the thrombin-induced inhibition of the Ca^{2+} wave propagation (comparision of black bars).

intercellular Ca^{2+} wave, we measured ATP levels in medium samples taken after initiation of the wave by MS using a bio-luminescent approach. A typical response (in counts) is shown in Fig. 2A ($N = 5$, $n = 10$). In order to investigate the exact effect of thrombin on Cx43-hemichannel-mediated ATP release after MS, we first measured the MS-induced ATP-release in a certain condition and afterwards we treated the same cells in the same chambered slide for 5 min with thrombin (2 U/ml). Then we applied again a mechanical stimulus and measured the ATP levels in the medium. By following this procedure, we are able to exactly compare the MS-induced ATP-release before and after thrombin treatment in each condition. The same procedure was applied for all conditions (i.e., control, TAT-Cx43CT, TAT-Cx43CT$^{DD/AA}$, TAT-CX43CT$^{RR/AA}$ and TAT-Cx43CT$^{PP/GG}$). Thrombin (2 U/ml for 5 min) markedly reduced ATP release upon MS ($N = 5$, $n = 10$) as described previously [18,20] and TAT-Cx43CT suppressed this inhibition. We further tested the effectiveness of TAT-Cx43CT$^{DD/AA}$, TAT-CX43CT$^{RR/AA}$ and TAT-Cx43CT$^{PP/GG}$ to suppress the thrombin-inhibition of ATP release following MS (Fig. 2B). TAT-Cx43CT$^{RR/AA}$ was equally potent in alleviating the thrombin-inhibition of ATP release following MS as TAT-Cx43CT, while TAT-Cx43CT$^{DD/AA}$ and TAT-Cx43CT$^{PP/GG}$ were ineffective in overcoming this thrombin-induced inhibition ($N = 5$, $n = 10$).

3.3. Asp and Pro residues are essential for TAT-Cx43CT to overcome high intracellular [Ca^{2+}]-induced inhibition of Cx43-hemichannel activity

Intracellular [Ca^{2+}] has a bimodal effect on Cx43-hemichannel activity, with [Ca^{2+}] elevation up to 500 nM peak amplitude triggering ATP release while higher [Ca^{2+}] inhibit ATP release [13–15,24,27]. Previously, we used the Ca^{2+} ionophore, A23187, to induce intracellular [Ca^{2+}] elevations in a controlled manner. Both in C6 glioma and HeLa cells that are ectopically expressing Cx43, 2 μM A23187 triggered cytosolic [Ca^{2+}] elevations in the 500 nM range, whereas 10 μM A23187 triggered cytosolic [Ca^{2+}] elevations in 1 μM range [14,24]. Here, we used HeLa cells ectopically expressing Cx43 and triggered intracellular increases in [Ca^{2+}] by using the Ca^{2+} ionophore A23187: 0.1 μM A23187 was unable to provoke ATP release, 2 μM A23187 provoked ATP release and 10 μM A23187 inhibited ATP release (Fig. 3A). TAT-Cx43CT completely abolished this inhibition of ATP release by 10 μM A23187 (Fig. 3A). TAT-Cx43CT$^{RR/AA}$ too alleviated the inhibition of Cx43 hemichannel-mediated ATP release, while TAT-Cx43CT$^{DD/AA}$ and TAT-Cx43CT$^{PP/GG}$ were not able to overcome the high intracellular [Ca^{2+}] inhibition. Similar findings were obtained with the reversed sequence of Cx43CT.

3.4. Asp and Pro residues are essential for TAT-Cx43CT to restore the activity of Cx43^{M239} hemichannels

Cx43^{M239}-based hemichannels fail to release ATP in response to cytosolic [Ca^{2+}] elevation to ~500 nM with 2 μM A23187, a condition known to activate Cx43 hemichannels composed of WT Cx43 [24] (Fig. 3B). Adding TAT-Cx43CT restored the impaired response of Cx43^{M239} hemichannels (Fig. 3B). We further examined the mutant versions of TAT-Cx43CT in their ability to restore Cx43^{M239}-hemichannel activity (Fig. 3B). Similar to our previous experiments, TAT-Cx43CT$^{RR/AA}$ was equally potent as TAT-Cx43CT, while TAT-Cx43CT$^{DD/AA}$ and TAT-Cx43CT$^{PP/GG}$ did not restore Cx43^{M239}-hemichannel activity.

3.5. Biotin-Cx43CT$^{DD/AA}$ fails to bind the CL domain of Cx43

Recently, we identified a cluster of nine positively charged aa in the CL domain as being sufficient for interaction with the C-terminal tail of Cx43 [15]. Therefore, we examined whether the two Aspartate residues in Cx43CT were critical for loop/tail interactions using SPR using the purified CL domain (Fig. 4A). We immobilized biotin-Cx43CT, biotin-Cx43CT$^{DD/AA}$ and biotin-Cx43CT reverse peptides to a streptavidin-coated sensor chip and applied different [CL] (Fig. 4B and C). The signal obtained using biotin-Cx43CT reverse was used as a reference channel and was subtracted from the signals obtained with biotin-Cx43CT (Fig. 4B) and biotin-Cx43CT$^{DD/AA}$ (Fig. 4C). Consistent with our previous reports [15,24], purified CL specifically bound to biotin-Cx43CT in a concentration-dependent manner (Fig. 4B). Importantly, binding of purified CL to biotin-Cx43CT$^{DD/AA}$ was compromised (Fig. 4C). We plotted the data from three independent runs and fitted the data using a Boltzmann function (Fig. 4D). Although we were unable to reach saturation values for this dose response curve, based on the fitted curve we estimate an EC50 in the range of 7–10 μM. In contrast, the binding of the purified CL domain to biotin-Cx43CT$^{DD/AA}$ was only evident at high concentration and was much lower than the binding to biotin-Cx43CT. The negative values in the SPR sensorgrams indicate that the CL domain displayed higher binding to the reverse sequence than to Biotin-Cx43CT$^{DD/AA}$. These data indicate that the two Asp residues in the Cx43CT peptide are critical for loop/tail interactions.

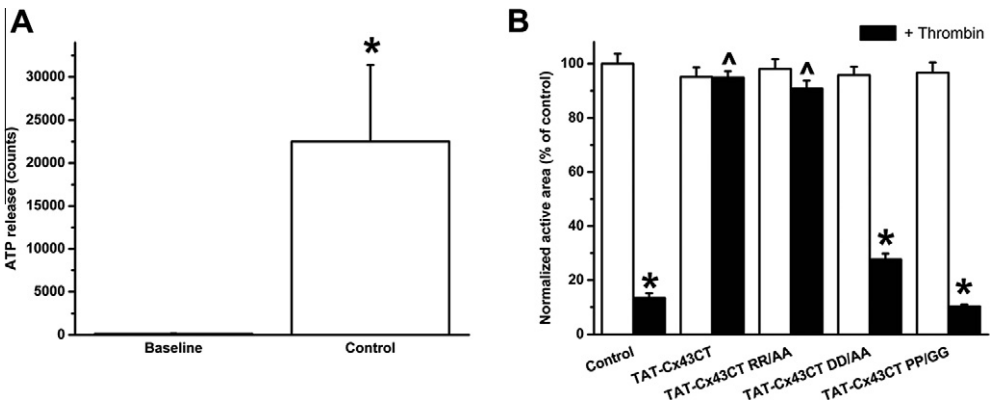

Fig. 2. Effect of TAT-Cx43CT, TAT-Cx43CT$^{RR/AA}$, TAT-Cx43CT$^{DD/AA}$ and TAT-Cx43CT$^{PP/GG}$ on the thrombin-induced inhibition of ATP release in BCEC. (A) Mean number of light counts under baseline (no stimulation) and after MS (control condition) were quantified ($N = 5$, $n = 10$). (B) Quantitative measurement of ATP release associated with the MS-induced intercellular Ca^{2+}-wave assessed by luciferin–luciferase bioluminescence. Normalized ATP release after MS of untreated (white bars) and thrombin-treated (black bars) BCEC, either in control conditions ($N = 5$, $n = 10$) or in conditions pre-treated with TAT-Cx43CT, TAT-Cx43CT$^{DD/AA}$, TAT-Cx43CT$^{PP/GG}$ or TAT-Cx43CT$^{RR/AA}$ ($N = 5$, $n = 10$), is shown. * indicates a significant ($p < 0.001$) inhibition compared to the untreated condition (white bars). ^ indicates that TAT-Cx43CT and TAT-Cx43CT$^{RR/AA}$ significantly ($p < 0.001$) alleviate the thrombin-induced inhibition of ATP release (comparision of black bars).

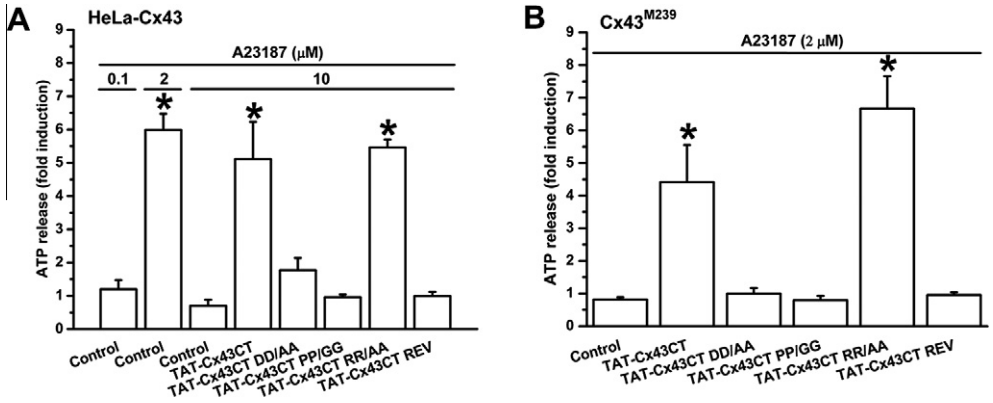

Fig. 3. (A) TAT-CX43CT and TAT-Cx43CT$^{RR/AA}$, but not TAT-Cx43CT$^{DD/AA}$ and TAT-Cx43CT$^{PP/GG}$, alleviate high cytosolic [Ca^{2+}]-induced inhibition of Cx43-hemichannel-mediated ATP release in Cx43-expressing HeLa cells. ATP release triggered from Cx43-expressing HeLa cells in response to 0.1 μM, 2 μM and 10 μM A23187 in untreated conditions or in response to 10 μM A23187 in cells pre-treated with TAT-Cx43CT, TAT-Cx43CT$^{DD/AA}$, TAT-Cx43$^{PP/GG}$ or TAT-Cx43CT$^{RR/AA}$. TAT-Cx43CT REV (TAT-Cx43CT reverse) represents the reversed sequence of Cx43CT fused to TAT. Values were obtained from six independent stimulations and show ATP release as fold induction of baseline values. (B) TAT-Cx43CT and TAT-Cx43CT$^{RR/AA}$, but not TAT-Cx43CT$^{DD/AA}$ and TAT-Cx43CT$^{PP/GG}$, are able to restore the activity of non-functional Cx43^{M239} hemichannels. ATP release triggered from Cx43^{M239}-expressing HeLa in response to 2 μM A23187 in untreated conditions or pre-treated with TAT-Cx43CT, TAT-Cx43CT$^{DD/AA}$, TAT-Cx43CT$^{PP/GG}$ or TAT-Cx43CT$^{RR/AA}$. Values were obtained from six independent stimulations and show ATP release as fold induction of baseline values.

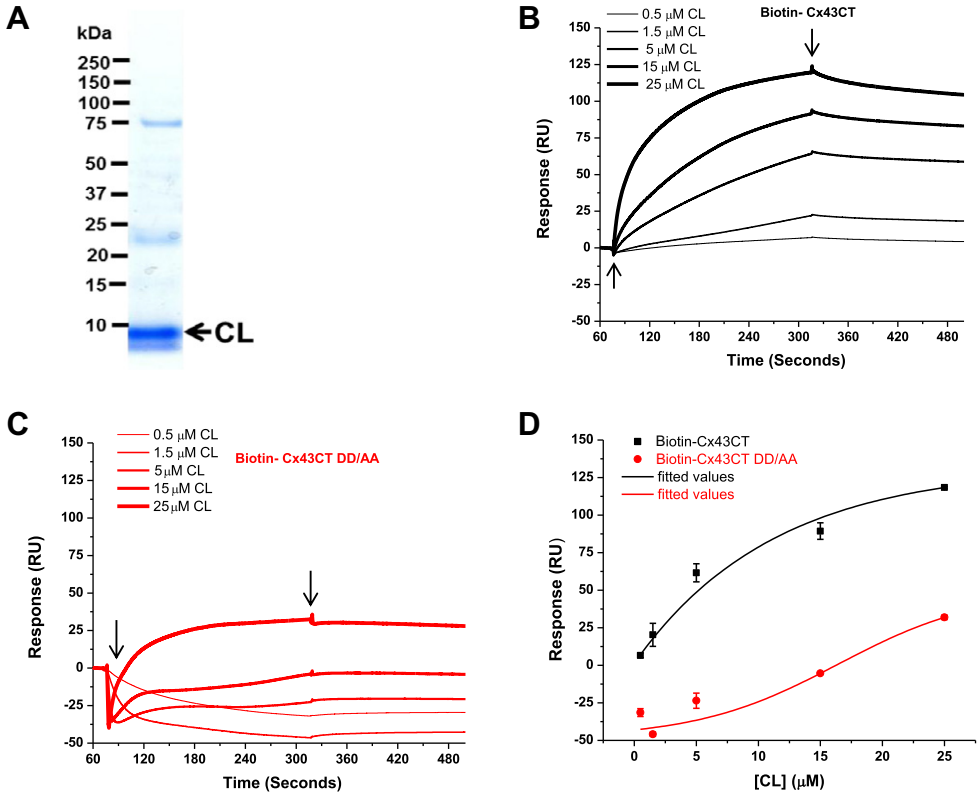

Fig. 4. The purified CL domain of Cx43 binds to biotin-Cx43 CT, but not to biotin-Cx43 CT$^{DD/AA}$, in SPR experiments. (A) A representative GelCode Blue-stained 4–12% Bis-Tris NUPAGE gel run in MES-SDS buffer showing the quality of the purified CL domain of Cx43 after glutathione-Sepharose 4B purification and PreScission protease cleavage. The arrow indicates the purified CL domain. (B and C) Typical sensorgrams in response units (RU) as function of time (seconds) representing the binding of purified CL domain (ranging from 0.5 μM to 25 μM) to biotin-Cx43CT peptide (B; black) or biotin-Cx43CT$^{DD/AA}$ peptide (C; red) immobilized to streptavidin-coated sensor chips. The arrows indicate the start of the association phase (first arrow) and the dissociation phase (second arrow). (D) Quantitative analysis of the binding of the CL domain to either biotin-Cx43CT (black) or biotin-Cx43CT$^{DD/AA}$ (red) based on the maximal RU values during the association phase. Values were obtained from reverse peptide-corrected sensorgrams of three independent experiments and are plotted as mean ± S.E.M. (For interpretation of color in this figure, the reader is referred to the web version of this article.)

4. Discussion

The last 10 aa sequence of the C-terminal tail of Cx43 (provided as TAT-Cx43CT) was identified as a domain that is essential for Cx43-hemichannel activity [24]. Using altered versions of TAT-Cx43CT, we identified two Asp and two Pro residues as the essential molecular determinants in controlling Cx43-hemichannel opening, while the two Arg residues were dispensable.

The seminal work of Delmar and co-workers on Cx43 gap junctions revealed a "ball-and chain" model for Cx43-gap junction gating [28–33]. The pH-dependent binding of the C-terminal tail to the L2 region of the cytoplasmic loop of Cx43 closes Cx43 gap junctions during acidification [33]. Similar interactions were found in Cx43 hemichannels but with a distinct outcome [24]. Indeed, intramolecular loop/tail interactions seemed required for obtaining functional Cx43 hemichannels. Removal of the C-terminal tail from

Cx43 ($Cx43M^{239}$) resulted in non-functional hemichannels, while TAT-Cx43CT restored the activity of these non-functional $Cx43^{M239}$-based hemichannels.

Here, we identified four aa as being critical, two Asp and two Pro residues. This correlates well with a study of Sorgen, identifying the residues in the C-terminal tail affected by the presence of CL in an NMR study [33]. We propose that the two Asp residues directly mediate the loop/tail interactions essential for establishing functional Cx43 hemichannels, while the two Pro residues likely are essential for the structural organization of the two Asp residues. This fits with our recent findings showing that a positively charged cluster of nine aa (the nonapeptide Gap19) is sufficient to bind the C-terminal tail of Cx43 [15]. In addition to intramolecular interactions with Cx43 CL domains, the C-terminal-most 10–12 aa of Cx43 are significant in mediating stable interactions with ZO-1 [34]. In turn, the Cx43CT-ZO-1 interaction is key to regulating the transition of connexons into gap junction channels [35,36]. Ongoing studies will determine whether this short CT sequence of Cx43 has further as yet unidentified interactions that depend on its conspicuous sequence of prolines and charged amino acid residues. In any case, for the direct regulation of Cx43 hemichannels by loop/tail interactions, Asp378 and Asp379 together with Pro375 and Pro377 seem to be crucial for rendering Cx43 hemichannels in an activatable state.

Acknowledgments

The work has been supported by Concerted Actions of the K.U. Leuven (GOA/09/012), the Research Foundation – Flanders (F.W.O.; grants G.0545.08 to BH and G.0298.11 to LL and GB) and Interuniversity Attraction Poles Program (Belgian Science Policy; P6/28 and P7/13 to G.B., and P6/31 and P7/10 to L.L.). CDH is a post-doctoral fellow of the Research Foundation – Flanders (FWO). We sincerely thank Dr. Elke De Vuyst for help with the ATP assays in HeLa cells.

References

[1] E. Scemes, S.O. Suadicani, G. Dahl, D.C. Spray, Connexin and pannexin mediated cell-cell communication, Neuron Glia Biol. 3 (2007) 199–208.
[2] H.S. Duffy, A.G. Fort, D.C. Spray, Cardiac connexins: genes to nexus, Adv. Cardiol. 42 (2006) 1–17.
[3] J.C. Saez, V.M. Berthoud, M.C. Branes, A.D. Martinez, E.C. Beyer, Plasma membrane channels formed by connexins: their regulation and functions, Physiol. Rev. 83 (2003) 1359–1400.
[4] W.H. Evans, E. De Vuyst, L. Leybaert, The gap junction cellular internet: connexin hemichannels enter the signalling limelight, Biochem. J. 397 (2006) 1–14.
[5] C. D'hondt, R. Ponsaerts, H. De Smedt, G. Bultynck, B. Himpens, Pannexins, distant relatives of the connexin family with specific cellular functions?, Bioessays 31 (2009) 953–974
[6] L. Leybaert, K. Braet, W. Vandamme, L. Cabooter, P.E. Martin, W.H. Evans, Connexin channels, connexin mimetic peptides and ATP release, Cell Commun. Adhes. 10 (2003) 251–257.
[7] N. Wang, M. De Bock, E. Decrock, M. Bol, A. Gadicherla, M. Vinken, V. Rogiers, F.F. Bukauskas, G. Bultynck, L. Leybaert, Paracrine signaling through plasma membrane hemichannels, Biochim. Biophys. Acta (2012).
[8] S. Finkbeiner, Calcium waves in astrocytes-filling in the gaps, Neuron 8 (1992) 1101–1108.
[9] P. Gomes, S.P. Srinivas, W. Van Driessche, J. Vereecke, B. Himpens, ATP release through connexin hemichannels in corneal endothelial cells, Invest. Ophthalmol. Vis. Sci. 46 (2005) 1208–1218.
[10] P. Gomes, S.P. Srinivas, J. Vereecke, B. Himpens, ATP-dependent paracrine intercellular communication in cultured bovine corneal endothelial cells, Invest. Ophthalmol. Vis. Sci. 46 (2005) 104–113.
[11] B.E. Isakson, W.H. Evans, S. Boitano, Intercellular Ca^{2+} signaling in alveolar epithelial cells through gap junctions and by extracellular ATP, Am. J. Physiol. Lung Cell. Mol. Physiol. 280 (2001) L221–228.
[12] K. Paemeleire, P.E. Martin, S.L. Coleman, K.E. Fogarty, W.A. Carrington, L. Leybaert, R.A. Tuft, W.H. Evans, M.J. Sanderson, Intercellular calcium waves in HeLa cells expressing GFP-labeled connexin 43, 32, or 26, Mol. Biol. Cell 11 (2000) 1815–1827.
[13] E. De Vuyst, E. Decrock, L. Cabooter, G.R. Dubyak, C.C. Naus, W.H. Evans, L. Leybaert, Intracellular calcium changes trigger connexin 32 hemichannel opening, EMBO J. 25 (2006) 34–44.
[14] E. De Vuyst, N. Wang, E. Decrock, M. De Bock, M. Vinken, M. Van Moorhem, C. Lai, M. Culot, V. Rogiers, R. Cecchelli, C.C. Naus, W.H. Evans, L. Leybaert, Ca^{2+} regulation of connexin 43 hemichannels in C6 glioma and glial cells, Cell Calcium 46 (2009) 176–187.
[15] N. Wang, E. De Vuyst, R. Ponsaerts, K. Boengler, N. Palacios-Prado, J. Wauman, C.P. Lai, M. De Bock, E. Decrock, M. Bol, M. Vinken, V. Rogiers, J. Tavernier, W.H. Evans, C.C. Naus, F.F. Bukauskas, K.R. Sipido, G. Heusch, R. Schulz, G. Bultynck, L. Leybaert, Selective inhibition of Cx43 hemichannels by Gap19 and its impact on myocardial ischemia/reperfusion injury, Basic Res. Cardiol. 108 (2013) 309.
[16] M. De Bock, M. Culot, N. Wang, M. Bol, E. Decrock, E. De Vuyst, A. da Costa, I. Dauwe, M. Vinken, A.M. Simon, V. Rogiers, G. De Ley, W.H. Evans, G. Bultynck, G. Dupont, R. Cecchelli, L. Leybaert, Connexin channels provide a target to manipulate brain endothelial calcium dynamics and blood-brain barrier permeability, J. Cereb. Blood Flow Metab. 31 (2011) 1942–1957.
[17] J. Stehberg, R. Moraga-Amaro, C. Salazar, A. Becerra, C. Echeverria, J.A. Orellana, G. Bultynck, R. Ponsaerts, L. Leybaert, F. Simon, J.C. Saez, M.A. Retamal, Release of gliotransmitters through astroglial connexin 43 hemichannels is necessary for fear memory consolidation in the basolateral amygdala, FASEB J. 26 (2012) 3649–3657.
[18] C. D'hondt, R. Ponsaerts, S.P. Srinivas, J. Vereecke, B. Himpens, Thrombin inhibits intercellular calcium wave propagation in corneal endothelial cells by modulation of hemichannels and gap junctions, Invest. Ophthalmol. Vis. Sci. 48 (2007) 120–133.
[19] C. D'hondt, R. Ponsaerts, S.P. Srinivas, J. Vereecke, B. Himpens, Reduced intercellular communication and altered morphology of bovine corneal endothelial cells with prolonged time in cell culture, Curr. Eye Res. 34 (2009) 454–465.
[20] C. D'hondt, S.P. Srinivas, J. Vereecke, B. Himpens, Adenosine opposes thrombin-induced inhibition of intercellular calcium wave in corneal endothelial cells, Invest. Ophthalmol. Vis. Sci. 48 (2007) 1518–1527.
[21] P. Gomes, S.P. Srinivas, J. Vereecke, B. Himpens, Gap junctional intercellular communication in bovine corneal endothelial cells, Exp. Eye Res. (2006).
[22] R. Ponsaerts, C. D'hondt, G. Bultynck, S.P. Srinivas, J. Vereecke, B. Himpens, The myosin II ATPase inhibitor blebbistatin prevents thrombin-induced inhibition of intercellular calcium wave propagation in corneal endothelial cells, Invest. Ophthalmol. Vis. Sci. 49 (2008) 4816–4827.
[23] R. Ponsaerts, C. D'hondt, F. Hertens, J.B. Parys, L. Leybaert, J. Vereecke, B. Himpens, G. Bultynck, RhoA GTPase switch controls Cx43-hemichannel activity through the contractile system, PLoS One 7 (2012) e42074.
[24] R. Ponsaerts, E. De Vuyst, M. Retamal, C. D'hondt, D. Vermeire, N. Wang, H. De Smedt, P. Zimmermann, B. Himpens, J. Vereecke, L. Leybaert, G. Bultynck, Intramolecular loop/tail interactions are essential for connexin 43-hemichannel activity, FASEB J. 24 (2010) 4378–4395.
[25] W.H. Evans, G. Bultynck, L. Leybaert, Manipulating connexin communication channels: use of peptidomimetics and the translational outputs, J. Membr. Biol. 245 (2012) 437–449.
[26] Y. Omori, H. Yamasaki, Gap junction proteins connexin32 and connexin43 partially acquire growth-suppressive function in HeLa cells by deletion of their C-terminal tails, Carcinogenesis 20 (1999) 1913–1918.
[27] M. De Bock, N. Wang, M. Bol, E. Decrock, R. Ponsaerts, G. Bultynck, G. Dupont, L. Leybaert, Connexin 43 hemichannels contribute to cytoplasmic Ca^{2+} oscillations by providing a bimodal Ca^{2+}-dependent Ca^{2+} entry pathway, J. Biol. Chem. 287 (2012) 12250–12266.
[28] H.S. Duffy, P.L. Sorgen, M.E. Girvin, P. O'Donnell, W. Coombs, S.M. Taffet, M. Delmar, D.C. Spray, pH-dependent intramolecular binding and structure involving Cx43 cytoplasmic domains, J. Biol. Chem. 277 (2002) 36706–36714.
[29] A.P. Moreno, M. Chanson, S. Elenes, J. Anumonwo, I. Scerri, H. Gu, S.M. Taffet, M. Delmar, Role of the carboxyl terminal of connexin43 in transjunctional fast voltage gating, Circ. Res. 90 (2002) 450–457.
[30] M. Delmar, W. Coombs, P. Sorgen, H.S. Duffy, S.M. Taffet, Structural bases for the chemical regulation of connexin43 channels, Cardiovasc. Res. 62 (2004) 268–275.
[31] H.S. Duffy, A.W. Ashton, P. O'Donnell, W. Coombs, S.M. Taffet, M. Delmar, D.C. Spray, Regulation of connexin43 protein complexes by intracellular acidification, Circ. Res. 94 (2004) 215–222.
[32] P.L. Sorgen, H.S. Duffy, P. Sahoo, W. Coombs, M. Delmar, D.C. Spray, Structural changes in the carboxyl terminus of the gap junction protein connexin43 indicates signaling between binding domains for c-Src and zonula occludens-1, J. Biol. Chem. 279 (2004) 54695–54701.
[33] B.J. Hirst-Jensen, P. Sahoo, F. Kieken, M. Delmar, P.L. Sorgen, Characterization of the pH-dependent interaction between the gap junction protein connexin43 carboxyl terminus and cytoplasmic loop domains, J. Biol. Chem. 282 (2007) 5801–5813.
[34] F. Xiao, J. Weng, K. Fan, W. Wang, Detailed regulatory mechanism of the interaction between ZO-1 PDZ2 and connexin43 revealed by MD simulations, PLoS One 6 (2011) e21527.
[35] J.M. Rhett, J. Jourdan, R.G. Gourdie, Connexin 43 connexon to gap junction transition is regulated by zonula occludens-1, Mol. Biol. Cell 22 (2011) 1516–1528.
[36] J.A. Palatinus, J.M. Rhett, R.G. Gourdie, The connexin43 carboxyl terminus and cardiac gap junction organization, Biochim. Biophys. Acta 2012 (1818) 1831–1843.